Thermal Annealing on P3HT/PC70BM Solar Cells Incorporated with Au and CuONanoparticales

Aruna P. Wanninayake, Shengyi Li, Benjamin C. Church, Nidal Abu-Zahra*

Department of Materials Science, University of Wisconsin-Milwaukee,

3200 North Cramer Street, Milwaukee, WI 53201, USA

(wannina2@uwm.edu, shengyi@uwm.edu, church@uwm.edu, nidal@uwm.edu)

*Correspondence should be addressed to: Nidal Abu-Zahra, Department of Materials Science, University of

Wisconsin-Milwaukee, 3200 North Cramer Street, Milwaukee, WI 53201, USA

Tel: +01 414 229-2668, nidal@uwm.edu

Abstract-In this work, thermal annealing is investigated to augment photovoltaic conversion efficiency (PCE) in bulk heterojunction polymer solar cells (BHJ-PSCs). Active layer (P3HT/PC70BM) and PEDOT: PSS films of these PSCs contain copper oxide nanoparticles (CuO-NPs) and gold nanoparticles (Au-NPs) respectively. Thermal annealing of P3HT/PC70BM thin films was performed at 150ºC for 30 minutes. X-ray diffraction (XRD) and differential scanning calorimetry (DSC) examination show an increased crystallinity of the heat-treated samples. Atomic force microscopic analysis (AFM) shows increased surface roughness after annealing, producing extra locations for crystallization of P3HT. Ultraviolet (UV)-visible as well as external quantum efficiency (EQE) spectra show enhanced self-organization, enhancing both crystallinity of P3HT and phase separation of the spin coated P3HT/PC70BM polymer films. However, ultraviolet-visible spectra do not show remarkable enhancement in light absorption with increasing gold concentration of PEDOT:PSS thin film owing to localised surface plasmonic resonance (LSPR) being distributed horizontally through the PEDOT:PSS film. PCE improved by 24% in the heat treated (Au/PEDOT: PSS)/(CuO/P3HT/PC70BM) solar cells.

1. Introduction

Polymer photovoltaic devices have been attracting attention in recent years as photo generating cells, owing to their simple device structure, easy fabrication, light weight together with optically and electronically adjustable molecular structure [1,2]. Bulk heterojunction (BHJ) PSCs benefit from a homogeneous donor-acceptor (D-A) contact interface compared to the inorganic counterpart. A homogenous D-A interface offers a longer free path for charge carriers, resulting in a longer diffusional pathway and a larger coulomb

interaction between electrons and holes. This is triggered by the low dielectric constant of organic semiconductors. Among various conventional donor-acceptor structures, poly(3-hexylthiophene)/[6,6]-phenyl-C70-butyric acid methyl ester (P3HT/PCBM) mixture is highly encouraging due to the unique properties of P3HT [3-5]. P3HT molecules possess superior charge transport ability $(1/10^4 – 1/10$ cm^2/V s) and crystallinity in bulk state as well as expanded photo-absorption and environmental stability. Several researchers have attempted enhancing the PCE in polymer based solar cells by various approaches. These include the design of novel device structures, producing materials with short energy gap, morphological refining of polymer thin films, upgrading photo generation ability, and creation of higher electron-hole mobility by adjusting D-A contact surface [6–9]. To enhance the molecular ordering and surface morphology in spun-casted polymer films, several strategies such as thermal/ solvent annealing [10–12] and using additives [13] have been used successfully. This in turn will increase light harvesting of P3HT:PCBM film and improve PCE. Motaung*et al.* [14] obtained 1.03% maximum PCE for ZnO incorporated P3HT: PCBM devices which were heat treated up to 140° C. Kang *et al.* [15] reported 3.86% PCE, 0.68V open-circuit voltage (V$_{oc}$) and 64% fill factor (FF) through post-annealing at 170 °C.

To improve the photon harvesting in PSCs, the incorporation of inorganic nanoparticles (INPs) has been extensively investigated. Nanoparticles (NPs); such as ZnO, TiO$_x$, and CdSe can be successfully incorporated into P3HT: PCBM layers as electron acceptors [16]; whereas Au and Ag NPs [17] have been used to enhance the photon absorbance. CuO NPs were successfully incorporated into the P3HT/ PC70BM active layer by our research group. The PCE of cells with 0.6 mg CuONPs increased by 40.9% due to enhanced carrier generation ability of P3HT: PCBM film [18, 19]. Meanwhile, a tremendous number of researches have been carried out on the incorporation of Au NPs in solar cells to investigate interfacial modifications for better charge carrier collection and enhancement of exiton dissociation. Chen *et al.* [20] reported 4.19% PCE with a 20% improvement in gold NPs (35nm) incorporated organic hybrid photovoltaic devices. Xie *et al.* [21] incorporated a relatively small Au NPs (18 and 35 nm in diameter) into PEDOT/PSS, P3HT/PCBM films, achieving 2.15% maximum PCE with 22% enhancement. The incorporation of Au NPs both in PEDOT/PSS [Poly(3/4ethylenedioxythiophene)poly (styrenesulfonate)] and active layers resulted in

~22% increase of PCE [22]. However, incorporation of Au NPs only in PEDOT/PSS [23] improved the PCE from 6.4% -7.6% with 18% enhancement due to the forward-scattering of NPs. However, Chen *et al.* [24] reported a strong near field surrounding gold NPs caused by LSPR which is distributed horizontally through PEDOT/PSS, resulting in marginal photon absorption increment of P3HT/ PC70BM film.

This study is focused on improving the power conversion efficiency of PSCs containing CuO NPs incorporated in P3HT/ PC70BM film and Au NPs in PEDOT:PSS film. For optimization of surface-morphology of P3HT/ PC70BM and PEDOT:PSS layers thermal annealing is considered as a convenient technique. XRD and UV–visible analysis were employed in studying morphological, structural and optical improvement in the CuO NPs/P3HT/PCBM-Au/PEDOT: PSS layers processed by thermal annealing. Outcome of heat-treated hybrid devices upon their electrical performance is presented in this work.

2. Experimental Methods

2.1 Materials

Under the same experimental conditions, a set of polymer based photovoltaic devices which were varying in their Au and CuO NPs content were fabricated and tested. P3HT was bought from Rieke Metals and PC70BM from SES Research. They were used as received. PEDOT/PSS mixed in distilled water was obtained from Sigma Aldrich and same amount of distilled water was added. Online purchasing (Nanocs, Inc) was done for conducting glass substrates (24 x 80 x 1.2 mm (12 Ω/cm^2) and conducting layer 25 to100nm). Au (18 nm diameter) and CuO (100 to 150nm diameter) NPs also were ordered online (nanocs.com). Airgas-company supplied purified N$_2$ gas and Al coils with a diameter of 0.15 mm were obtained online (Ted-Pella).

2.2 Fabrication of solar cells

The fabrication of Polymer based solar cells containing gold and copper oxide NPs was done in a glove box usingN$_2$ as the inert atmosphere. The P3HT: PCBM:CuO NPs blendswereobtained in two-steps.First, the P3HT-PC70BM blend was obtained by diluting same amount ofregioregular P3HT and PC70BM (10 mg each) with 2ml of chlorobenzene (C$_6$H$_5$Cl) andmixed constantly for 14 hours at a temperature of 60º C.CuO NPs also were dispersed in the same volume of C$_6$H$_5$Cl and added to the above

mixture, so that weight ratios of ingredients (P3HT/PCBM/CuO-NPs) in the final blend was 10:10:0.6 mg. In addition, different amounts of Au NPs were added to 10 ml of PEDOT: PSS aqueous solution, leading to six PEDOT: PSS solutions with 0, 0.02, 0.06, 0.10, 0.14, and 0.18 mg of NPs; respectively.

The solar cell device structurethat wasspuncoatedin this research is schematically presented in figure 1. In a glove box with N_2environment, the solar cell devices were spuncoated by installing the PEDOT/PSS film on a conductive glass plate and P3HT/PC70BM film on the top of it. Using ultrasonic cleaning method, the conducting glass substrates were cleaned with ammonium hydroxide, hydrogen peroxide, distilled water, methyl alcohol, and isopropyl alcoholsuccessively. The 40 nm-thick PEDOT/PSS/Au layers, which serveas thin hole-transport layers, were prepared by spun-coating at rotational velocity of4000rpm followed by heating at 120°C for 20 minutes in air. After the temperature of the samples came back to ambient temperature, the blends with P3HT:PC70BM: CuONPswere spun coated at 1000 rpm for one to two minutes.
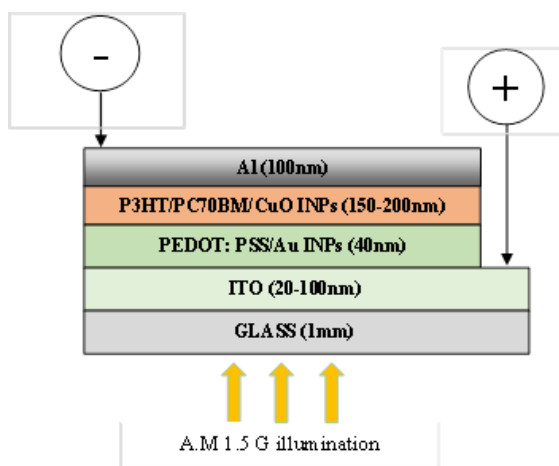

Fig.1. Graphical representation of the hybrid device architecture

This active layer had 120 nm average thicknesses and the device had $0.12cm^2$ surface area. Annealing was performed on all devicesinside an inert ovenfor 30 minutesafter Al electrode deposition. The annealing temperature was 150°C [18, 19].

2.3 Characterization

Under the general laboratory environment, the electronic and thermal behaviour of PSCs with a constant CuO NP content and different amount of Au NPs were analysed. Current density–voltage (J-V) characterization was carried for all PSCs. UV solar simulator consists of AM 1.5G filter and lamp (xenon lamp, Oriel Instruments) intensity of 100 mW/cm^2 was used. A source meter (Keithley 2400) was employed to obtain the J-V measurements. Device parameters such as short circuit current density (J_{sc}), open circuit voltage (V_{oc}), Fill Factor (FF) and power conversion efficiency were recorded in the PSCs containing varying amounts of gold NPs under ambient environment. A quantum efficiency measurement kit (Newport- serial number 425) embedded in the solar cell simulator was used to obtain EQE values. Merlin monochromator with a 300W Xenon arc lamp was used as a light source to provide throughput to the cells in the experiment.

The optical properties of samples containing varying amounts of gold NPs were obtained using a PerkinElmer LAMBDA 650 spectrophotometer. Crystallinity studies of the thin layers were performed with a Bruker D8 XRD with a Cu/K-α source under 40kV and 40mA tube current at a rate of 0.2° per minute. Recorded range of the X-ray spectra were from 4° - 7°. Differential scanning calorimetry spectra were obtained using a TA instruments Q2000 with 5°C per minute heating rate. DSC samples had a weight range of 8-12 mg and nitrogen gas flow rate to the DSC was 50 ml/min. An Agilent 5420 atomic force microscope (AFM) was used to analyze the surface morphology. The Pico Image Basics and Gwyddion software were utilized to determine the root mean square roughness (σ_{rms}) of surface under ACAFM noncontact mode with set point 1.60, I-gain of 10 and scanned area of 2x2μm [18, 19].

3. Results and Discussion

3.1 Morphological analysis

Interface morphology between PEDOT:PSS, P3HT/PCBM and electrodes has a crucial role in defining electrical properties of PSCs. Therefore, morphological regulation of thin layers of bulk heterojunction devices is essential to enhance the energy conversion efficiency. Thermal annealing causes alterations in morphology of polymer thin films. These changes were studied by AFM illustrations of Au/PEDOT:PSS-P3HT/PCBM/CuO

layers pre and post annealing at 150ºC for 30 minutes.

At the I-gain value of 10 and set-point value of 1.24, surface morphological studies of thin films were carried out for 2x2 μm sample area under AC-

AFM non-contact mode. The AFM morphology of PEDOT: PSS films containing different amounts of Au NPs, before thermal annealing, is shown in Figure 2. This illustrates that surface becomes rougher than

Fig. 2.AFM illustrations of PEDOT: PSS layers with different concentrations of Au NPs before annealing. (a) 0mg
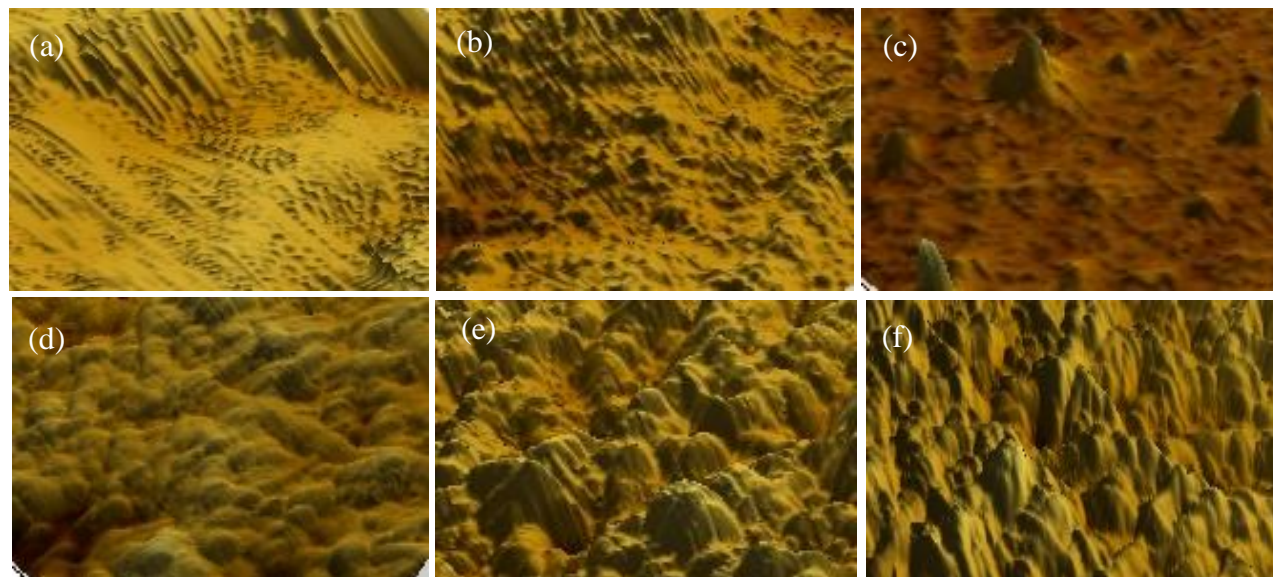
(b) 0.02mg (c) 0.06mg (d) 0.10mg (e) 0.14mg (f) 0.18mg

the controls proportionate to the concentration of Au NPs in layers. The σ_{rms} of the control layers was 0.36 nm and it was enhanced to 1.24 nm in the samples containing 0.18 mg of gold NPs.

However, samples subjected to thermal annealing did not show a significant improvement of surface roughness compared to those without annealing. The square-roughness of the optimum cell (containing 0.06 mg of Au NPs) was 0.88 nm.

Figure 3 indicates the effect of annealing on P3HT/PCBM thin films containing various concentrations of CuO NPs. AFM topography of these thin films displays coarser surface spikes compared to reference cells without CuONPs.The highest σ_{rms} value of layers containing 1mg CuO NPs was 0.43 nm compared to 0.15 nm in the layers with no CuO NPs. The best performed device having a CuO NPs concentration of 0.6mg showed a σ_{rms} of 0.34nm. After thermal annealing of thin films containing P3HT/PCBM/CuO NPs at 150°C over 30 minutes, surface roughness of thin films without CuO NPs was 0.43 nm and it increased up to 1.01 nm in the thin films with 1mg of CuO NPs. The heat treated cells with 0.6 mg of optimum CuO NPs concentration

exhibited a 0.82 nm σ_{rms} value. The enhanced roughness with thermal annealing could be attributed to improved microscopic phase separation between amorphous P3HT donor and amorphous PC70BM acceptor molecules.

It is expected that higher roughness of the thin film layers (PEDOT:PSS and P3HT/PCBM) provides a larger contact surface in the interface at Au/PEDOT:PSS-P3HT/PCBM/CuO NPs layers which will boost charge collection efficiency at electrodes yielding a higher power conversion efficiency [25]. The charge carrier diffusion length in the polymer thin films is a critical factor and it should be limited to a few nanometers. The charge carriers which are generated close to the electrodes can be converted easily into photocurrent.

The XRD patterns (Figure 4a), exhibit an improved self-organization of P3HT with incorporation of CuO NPs into the P3HT/PCBM thin films. The diffraction peaks intensities observed at $2\theta = 5.4º$ for P3HT: PC70BM: CuO NPs thin films are related to the well-organized P3HT molecular structure. P3HT molecules which were liberated from amorphous phase in the presence of Cu NPs and reorganized as

separate molecules within polymer blend could be the reason for this diffraction peaks which are observed in the samples before annealing. However, XRD peaks were not observed for PEDOT:PSS thin filmsbefore or after incorporating gold NPs. It could be due to the fact that these thin films did not have a significant crystallinity.
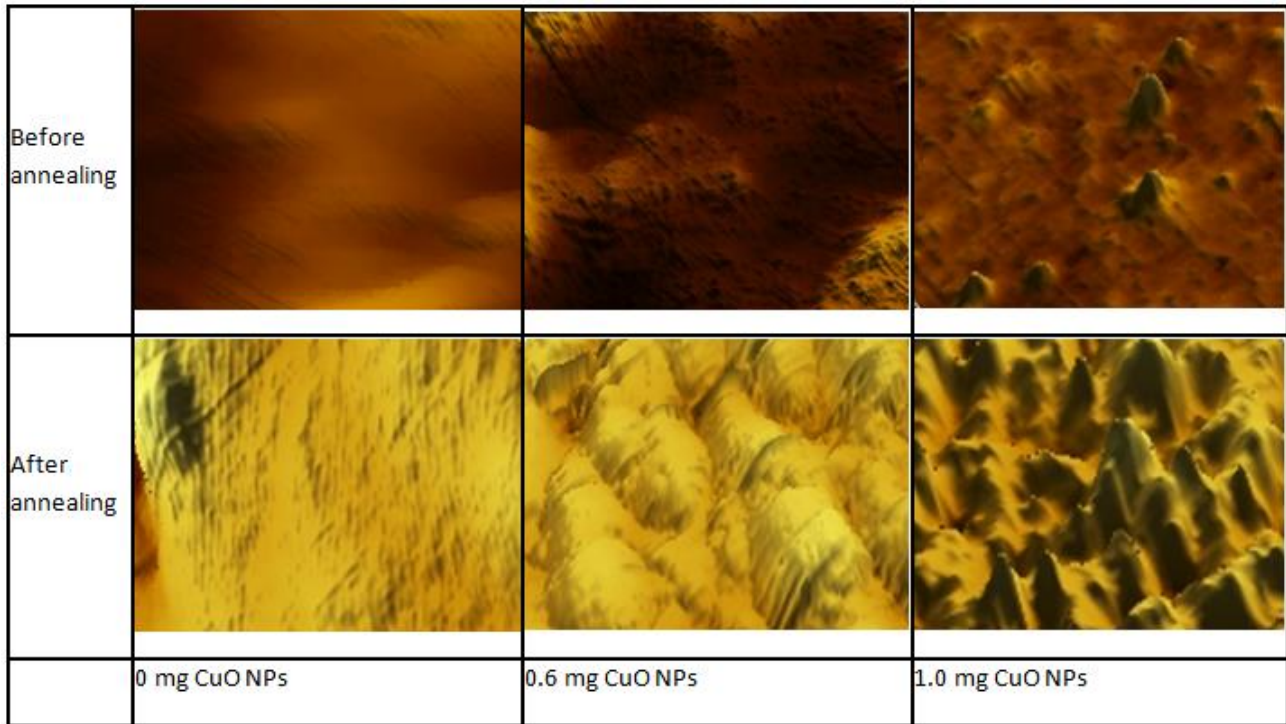

Fig. 3. AFM surface morphology of P3HT/PCBM thin films (pre and post annealing) with different amounts of CuO NPs
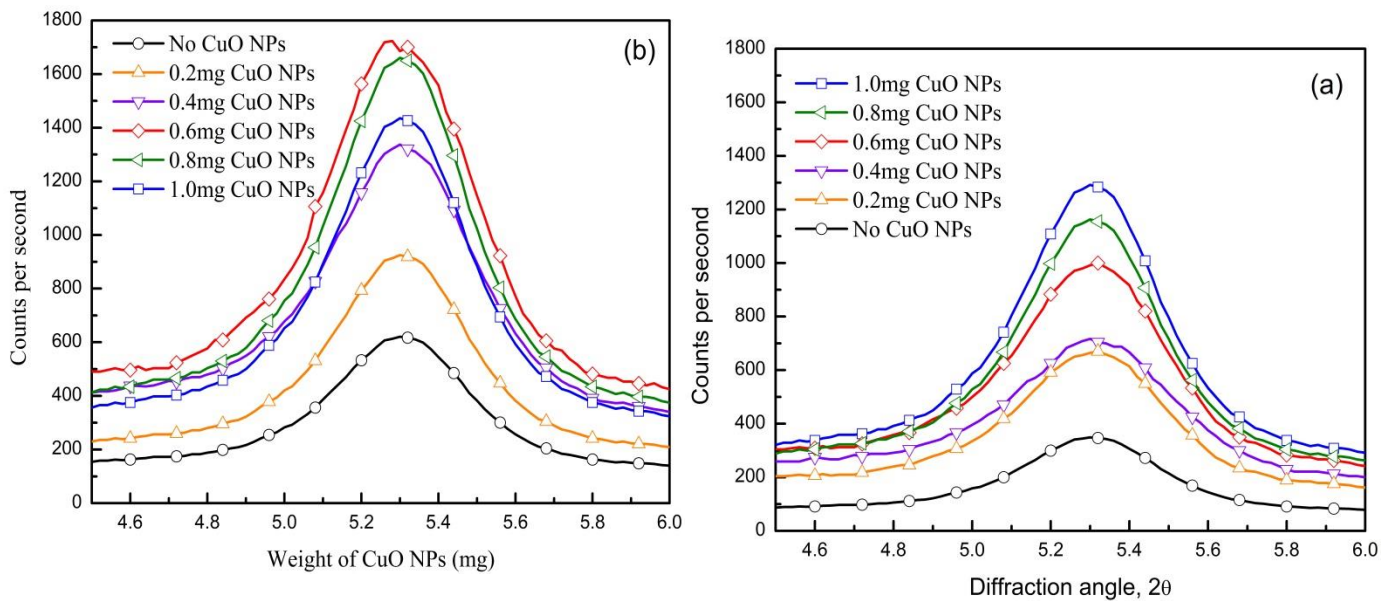
Fig. 4. XRD spectra for CuO NPs incorporated P3HT/PCBM thin films (a) pre annealing (b) post annealing

The XRD patterns (Figure 4a), exhibit an improved self-organization of P3HT with incorporation of CuO NPs into the P3HT/PCBM thin films. The diffraction peaks intensities observed at $2\theta = 5.4º$ for P3HT: PC70BM: CuO NPs thin films are related to the well-organized P3HT molecular structure. P3HT molecules which were liberated from amorphous phase in the presence of Cu NPs and reorganized as separate molecules within polymer blend could be the reason for this diffraction peaks which are observed in the samples before annealing. However, XRD peaks were not observed for PEDOT:PSS thin films before or after incorporating gold NPs. It could be due to the fact that these thin films did not have a significant crystallinity.Figure 4(b) indicates XRD patterns of post annealed devices. The evident increase in P3HT crystallinity may be attributed to further enhancement of self-organization with heat treatment. Being a fully amorphous material, PC70BM did not give significant diffraction peaks both with and without CuO NPs.

Hence, it can be concluded that only P3HT crystallization is affected by the addition of CuO NPs and thermal annealing but there is no effect on PC70BM crystallinity as it is a fully amorphous material [26]. The annealed samples with CuO NPs concentration of 0.6mg exhibited the maximum crystallinity. Further increasing the concentration of CuO NPs beyond 0.6 mg, resulted in a decrease of crystallinity. This can be attributed to aggregation and inadequate diffusing of CuO nanoparticles in the polymer blend, uncontrolled phase separation and disruption of P3HT molecular organization [27]. As presented in Figure 5, annealing increases the intensity of diffraction peaks of hybrid devices containing various concentrations of CuO NPs.
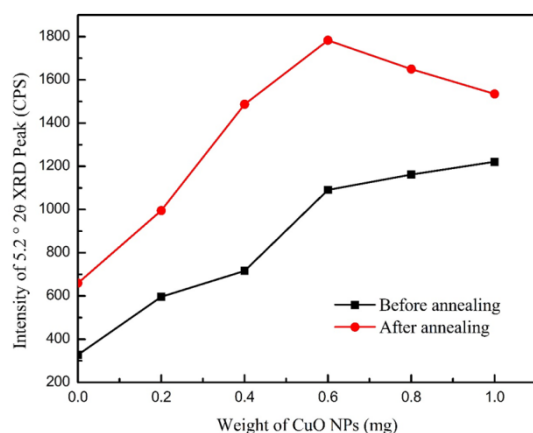
Fig. 5.XRD Diffraction peak intensity before and after annealing

Differential Scanning Calorimetry (DSC) was used to further investigate the relationship between annealing treatment and crystallinity of P3HT:PC70BM. Equation 1 was used to calculate the percentage crystallinity (X_c) of P3HT phase in the P3HT:PC70BM:CuO NPs active layer.

$$\% \, \boldsymbol{Crystallinity} \, (\boldsymbol{X_c}) = \left(\frac{\Delta H_m - \Delta H_c}{\Delta H}\right)\boldsymbol{100} \qquad (1)$$

Where ΔH_mindicates the melting enthalpy (in J/g of sample) of half-crystalline polymer in the mixture, $\Delta H_c$and$\Delta H$are the enthalpies of crystallization and melting of fully-crystalline polymer (ΔH of P3HT=99 J/g) [15] respectively.

As shown in Figure 6, the crystallinity percentage improves slowly with increasing CuO NPs concentration in P3HT/PC70BM structure, before annealing. Nevertheless, it has remarkably enhanced after annealing treatment. This behaviour can be due to P3HT/PC70BM phase separation and recrystallization of P3HT as single molecules. When the amount of CuO NPs was increased higher than 0.6mg the percentcrystallinity of the annealed samples began to decline. It is clearly eveident that
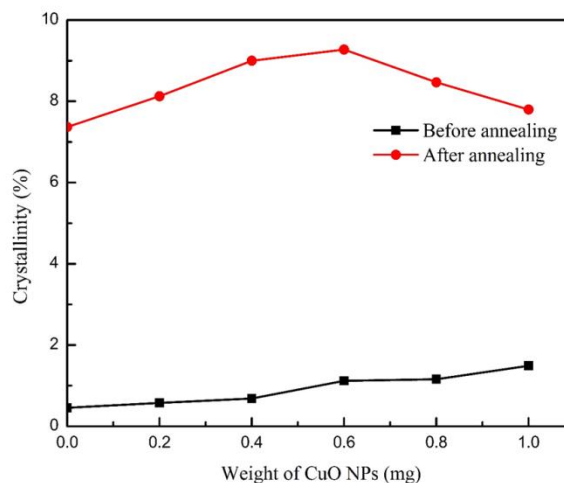
crystallinity data obtained by both XRD and DSC are comparable.

The UV visible absorption spectra of the Au/PEDOT:PSS and P3HT/PC70BM/0.6mg CuO NPs blend films were obtained to further explain the outcome of heat treatment on the optical properties of PSCs. The absorption intensities of all Au NPs incorporated solar cells improved after thermal annealing. This increased absorption intensities are attributed to the enhanced crystallinity of P3HT by annealing treatment combined with improved optical absorption caused by CuO NPs incorporated in P3HT/PC70BM layer. However, the absorption spectrum of PEDOT:PSS/P3HT:PCBM/0.6 mg CuO NPs solar cells did not show any significant improvement with increase of Au NPs concentration in the PEDOT:PSS thin film, as shown in Figure7. This can be attributed to the strong near field surrounding the Au NPs due to the LSPR which is distributed horizontally through the PEDOT:PSS thin film, instead of penetrating upward into the P3HT/PC70BM layer,thus causing less optical absorption [28].
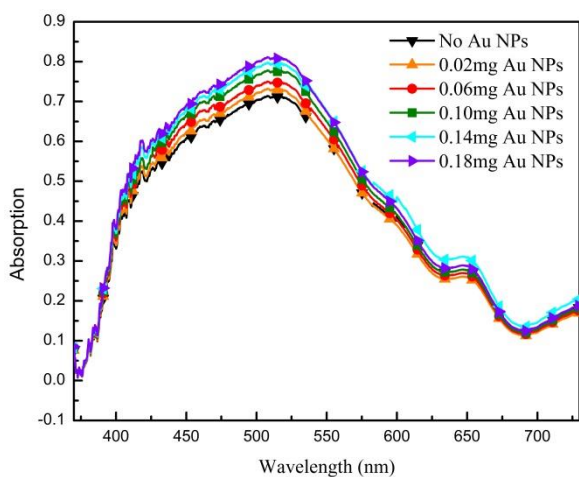

Fig. 7.Optical absorption spectra of annealed PSCs with Au NPs incorporated PEDOT: PSS

The EQE measurers the ratio between the incident photons on the solar cell from the input source and the generated free electron hole pairs by the device.Table 1 shows peakEQE values for annealed and non-annealed devices containing different concentrations of Au NPs.

The EQE spectrum improved over the wavelength range of 350 - 620 nm. Before annealing

Fig. 6. Crystallinity measurements using DSC before and after annealing

Au NPs (mg)	EQE (%)	
	Before annealing	After annealing
0	53	60
0.02	57	60
0.06	61	69
0.10	55	62
0.14	48	52
0.18	38	40

Table 1. The EQE measurements of Au/PEDOT: PSS/P3HT/PCBM/CuO-NP devices before and after annealing

the devices with 0.18, 0.14, 0.10, 0.06 and 0.02 mg of Au NPs had highest EQEs of 38%, 48%, 55%, 61% and 57% respectively, while that of the reference cell was 53%.However, after annealing the maximum values of the EQE spectra increased in all the devices to 40%, 52%, 62%, 69%, 60% and 60% respectively, as illustrated in Figure 8. The Au NPs which are incorporated in PEDOT:PSS thin film have a major effect on enhancing the hole collection ability of solar cells. The EQE enhancement is brought about by an increase of three factors, namely charge motilies, hole collection as well as light absorption [29, 30]. Therefore, it can be concluded that enhanced crystallinity, due to thermal annealing and electrical effects such as charge collection, charge mobility and exciton dissociation due to Au NPs, are more crucial than the plasmonic effects. However, at higher concentrations of Au NPs, the EQE starts to decrease. The reason behind this could be the excess amount of Au diffusing into the active layer and changing the P3HT/PCBM nanoscalemorphology which leads to minimization of the exciton dissociation.
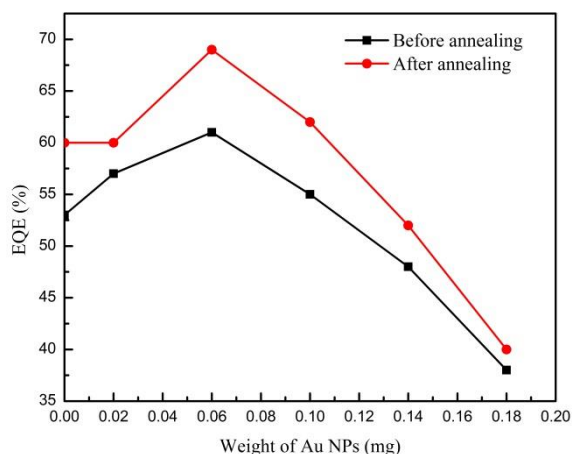
Fig. 8. Effect of annealing on the EQE values of PSCs with Au NPs

Table 2 summarizes the measured photovoltaic parameters, which are J_{sc}, V_{oc}, FF and PCE of all fabricated devices. PSCs were annaeled at a temperature of 150°C which exceeds the glass transition temperature of P3HT. There was a significant improvement of all the parameters following heat treatment.

The J-V characteristics measurements of devices without annealing revealed a J_{sc} of 6.484 mA/cm^2 in the control celland it increased to 7.491 mA/cm^2 in cells incorporated 0.06 mg of Au NPs with a 15.5% increment. This enhanced short circuit current improved PCE from 2.96% - 3.51%. Fill factor of the device increased from 68 to 69.21% and the open-circuit voltage (V_{oc}) did not change by adding gold NPs. Gold NPs incorporated in PEDOT:PSS thin film contributed for about 18% increase in PCE as a result of notably improved J_{sc} and FF. There was a drastic improvement of PCE with increasing Au NPs concentration in the PEDOT: PSS thin film up to 0.06 mg and then started to decrease beyond this point.

However, after thermal annealing the trend of V_{oc} did not change with increasing the amount of Au NPs in PEDOT:PSS; whereas J_{sc} improved from 7.996 to 9.092 mA/cm^2 and FF increased from 68.26% to 70.11%. Consequently, PCE elevated to

4.34% from 3.70%, leading to a 17% enhancement in the cells containing 0.06 mg of gold nanoparticles. J_{sc} enhancement also closely follows the EQE pattern. Based on power conversion efficiency equation (PCE = V_{oc}*J_{sc}*FF/total incident power density) V_{oc}, J_{sc}, and FF are significant factors in determining the overall PCE. Higher V_{oc}, J_{sc}, and FF result in higher PCE. The PCE values of the CuO NPs incorporated solar cells before and after annealing are shown in Figure 9.
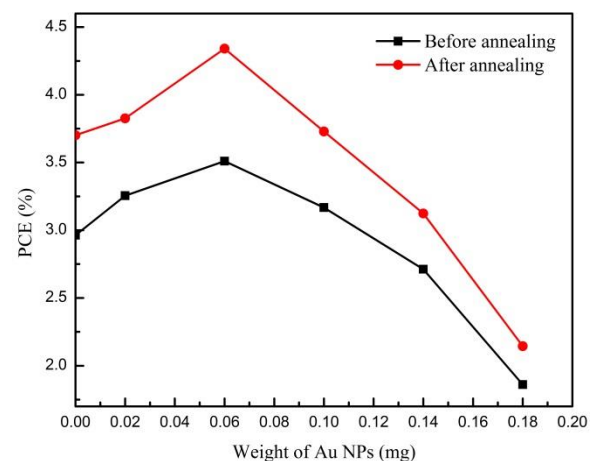

Fig. 9.PCE of the Au/PEDOT:PSS/P3HT/PCBM/CuO-NP hybrid devices before and after annealing

Open circuit voltage (V_{oc}) has a linear relationship to energized band levels within D-A phases. The linear correlation of the V_{oc} to the energetic gap between donor's HOMO level and acceptor's LUMO level can be shown as equation 2 [31, 32].

$$V_{oc} = E_{g,D/A} = E_{g,D} - (LUMO_D - LUMO_A)$$

(2)

The open circuit voltage (V_{oc}) did not change significantly, possibly since the LUMOs of P3HT and PC70BM were constant. Hence, V_{oc} had no effect on PCE increment in these cells [33, 34]. In contrast, J_{sc} of the annealed samples has significantly increased. This could be due to higher crystallinity leading to superior charge movability [35-37]. The annealing treatment of P3HT near the glass transition rearranges the molecular organization in the blend. This increases the charge propagation through P3HT to PCBM molecules, thus improving J_{sc} in the photovoltaic cells. Further, adding Au and CuO

nanoparticles to PEDOT:PSS and P3HT/PCBM thin films, produce hopping sites for the holes resulting in a higher hole mobility. This process also contributes to the enhanced J_{sc}. The fill factor (FF) remained nearly the same after annealing.Kim *et al.* [38]

suggested that the gold NPs produce hopping sites in polymer structures resulting in a higher hole mobility.

Au NPs (mg)	$J_{sc}(mA/cm^2)$		$V_{oc}(V)$		FF(%)		PCE(%)	
	Before heating	*After heating*	*Before heating*	*After heating*	*Before heating*	*After heating*	*Before heating*	*After heating*
0	6.484	7.996	0.673	0.678	68.00	68.26	2.963	3.701
0.02	7.006	8.176	0.678	0.679	68.52	68.92	3.255	3.826
0.06	7.491	9.092	0.677	0.681	69.21	70.11	3.510	4.341
0.10	6.901	8.025	0.685	0.680	67.02	68.33	3.168	3.729
0.14	5.984	6.921	0.671	0.672	67.54	67.17	2.712	3.124
0.18	4.195	4.752	0.673	0.677	65.91	66.64	1.861	2.144

Table 2. Performance parameters of Au/PEDOT:PSS/P3HT/PCBM/CuO-NP hybrid solar cells pre and post heat treatment
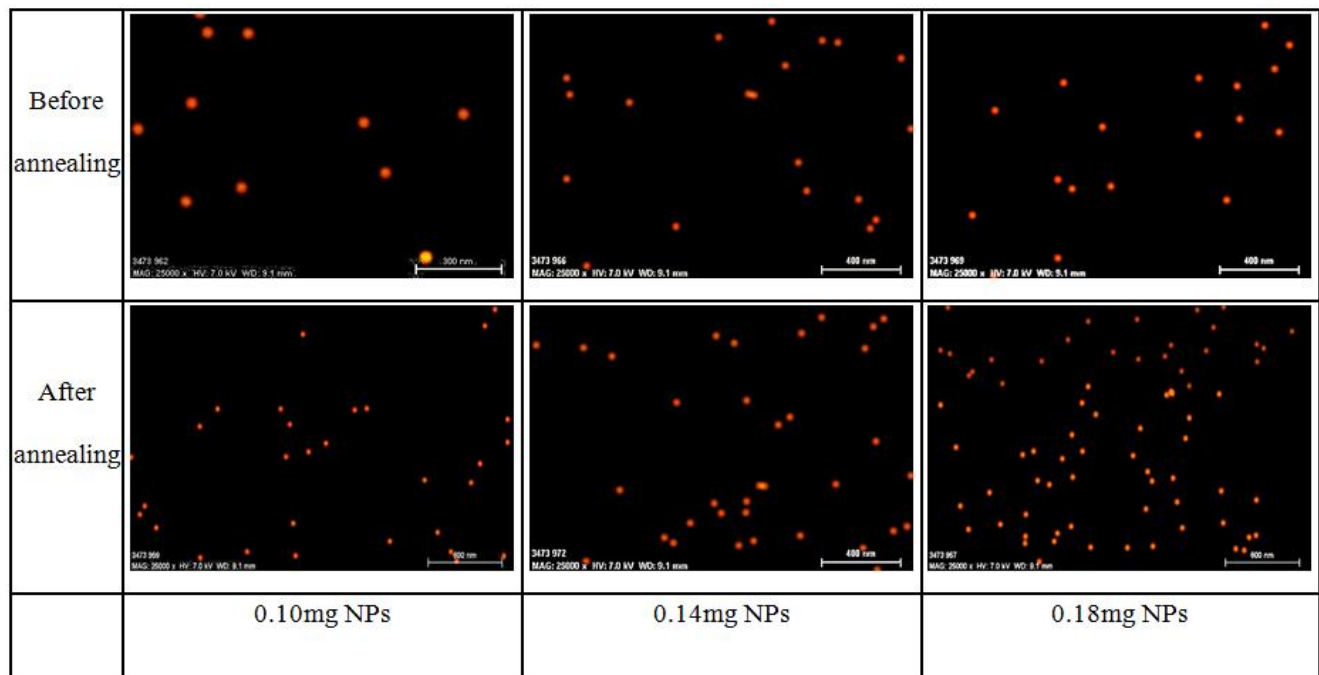

Fig. 10.EDX mapping showing the dispersion of gold NPs penetrated into thin active film before and after annealing

However, further increase of Au NPs, This morphology change causes a significant reduction of donor/acceptor contact surface. The modified donor/acceptor contact surface proportionally affects the excitonic dissociation [39], thus lowering the EQE and $J_{sc}$of the cells.

4. Conclusion

In this work, P3HT/PC70BM polymer blends were prepared adding 0.6mg of CuO NPs to increase P3HT crystallization as well as to improve the phase separation ability of P3HT/PC70BM. The PEDOT: PSS layer was tuned by adding Au NPs (0-0.18mg) to enhance the charge collection ability. EQE analysis and UV Visible absorption spectra exhibited improvement of self-organization ability and crystallization of P3HT. EQE of the solar cells increased due to increased charge collection at the electrodes. However, since the near field surrounding Au NPs caused by LSPR effect is distributed horizontally through PEDOT:PSS film, there is no significant improvement in light absorption with increasing the amount of Au NPs in PEDOT:PSS thin film. AFM analysis indicates a higher σ_{rms} of cells containing CuO NP, which indicates a larger space for P3HT crystallization. Increasing the P3HT crystallization discourages dissolving of PCBM within P3HT phases, thereby separating PC70BM phases from PC70BM/P3HT domain. At the annealing conditions of 150ºC for 30 minutes, Au/PEDOT:PSS/ P3HT/PC70BM/CuO solar cells exhibited 24% improvement in PCE due to increased photo absorption with elevated exciton generation rate, and enhanced hole electron mobility and charge transport due to improved crystallinity.

References

[1] N. Abu-Zahra, and M. Algazzar, Abu-Zahra, N. Algazzar, M.: "Enhancing Power Conversion Efficiency of P3HT/PCBM Polymer Solar Cells" International Journal of Chemical, Nuclear, Metallurgical and Materials Engineering. 8 (4), pp248-253, 2014.

[2] S.I. Na, D.P. Park, S.S.Kim, S.Y. Yang, K. Lee, M.H Lee "ITO-free flexible polymer solar cells with ink-jet-printed Ag grids"Semicond. Sci. Technol. 27 125002, October, 2012.

[3] W. Shen, J. Tang, R. Yang, H. Cong, X. Bao, Y. Wang, X. Wang, Z. Huang, J. Liu, L. Huang, J. Jiao, Q. Xu, W. Chenb, and L. A. Belfiore,"Enhanced efficiency of polymer solar cells by incorporated Ag–SiO2 core–shell nanoparticles in the active layer". RSC Advances. 4, pp 4379-4386, November, 2014.

[4] A. Konkin, C. Bounioux, U. Ritter, P. Scharff, E.A. Katz, A. Aganov, G. Gobsch, H. Hoppec, G. Ecke, H.K. Roth, "ESR and LESR X-band study of morphology and charge carrier interaction in blended P3HT–SWCNT and P3HT–PCBM–SWCNT solid thin films", Synthetic Metals. 161, pp2241–2248, September, 2011

[5] S. Jin, B.V.K. Naidu, H. Jeon, S. Park, , J. Park, S.C. Kim, J.W. Lee, and Y. Gal, "Optimization of process parameters for high-efficiency polymer photovoltaic devices based on P3HT: PCBM system. Solar Energy Materials and Solar Cells". 91, pp1187–1193, 2007

[6] A.Wicklein, S.Ghosh, M.Sommer, F.Wurthner, M.Thelakkat, "Self-Assembly of Semiconductor Organogelator Nanowires for Photoinduced Charge Separation" ACS Nano 3 (5), pp 1107–1114, May, 2009.

[7] M. Jorgensen, K.Norrman, F.C.Krebs, "Stability/degradation of polymer solar cells",Sol. Energ. Mat. Sol. Cells, 92, pp 686–714, March, 2008.

[8] T.Oyamada, C.Maeda, H.Sasabe, C.Adachi, "Efficient Electron Injection Mechanism in Organic Light-Emitting Diodes Using an Ultra-Thin Layer of Low-Work-Function Metals" Japanese Journal of Applied Physics 42, December, 2003

[9] F. Padinger, R.S. Rittberger, N.S. Sariciftci, "Effects of Postproduction Treatment on Plastic Solar Cells"Adv. Funct. Mater. 13, pp85-88, January 2003.

[10] W.H. Lee, S.Y. Chuang, H.L. Chen, W.F. Su, and C.H. Lin, "Exploiting optical properties of P3HT: PCBM films for organic solar cells with semitransparent anode"Thin Solid Films. 518, pp7450–7454 7450, May, 2010

[11] Y. Kim, S.A. Choulis, J. Nelson, D.D.C. Bradley, S. Cook, J.R. Durrant," Composition and annealing effects in polythiophene/fullerene solar cells" J. Mater. Sci. 40,pp 1371-1376, March 2005.

[12] G. Li, Y. Yao, H. Yang, V. Shrotriya, G. Yang, Y. Yang, "Solvent Annealing" Effect in Polymer Solar Cells Based on Poly(3-hexylthiophene) and Methanofullerenes"Adv. Funct. Mater. 17, pp 1636–1644, July, 2007

[13] T. Salim, L.H. Wong, B. Brauer, R. Kukreja, Y. L. Foo, Z. Bao, Y. M Lam, "Solvent additives and their effects on blend morphologies of bulk heterojunctions" J. Mater. Chem., 21, pp 242-250, October, 2011

[14] D. E. Motaung, G. F. Malgas, S. S. Ray, C. J. Arendse, "Annealing effect of hybrid solar cells based on poly (3-hexylthiophene) and zinc-oxide nanostructures" Thin Solid Films 537, pp 90-96, April, 2013

[15] R. Kang, S. Oh, S. Na, T. S. Kim, D. Y. Kim, "Investigation into the effect of post-annealing on inverted polymer solar cells" Sol. Energ. Mat. Sol. Cells, 120, pp 131-135, January 2014.

[16] W. J. E. Beek, M. M. Wienk, and R. A. J. Janssen, "Efficient Hybrid Solar Cells from Zinc Oxide Nanoparticles and a Conjugated Polymer" Adv. Mater. 16, pp 1009–1013, June 2004.

[17] H. Liao, C. Tsao, T. Lin, M. Jao, C. Chuang, S, Chang, Y. Huang, Y. Shao, C. Chen, C. Jeng, Y. Chen, and W. Su, "Nanoparticle-tuned self-organization of a bulk heterojunction hybrid solar cell with enhanced performance" ACS Nano, 6, pp 1657-1666, January 2012

[18] A. P. Wanninayake, S. Gunashekar, S. Li, B.C. Church and N. Abu-Zahra,"CuO Nanoparticles Based Bulk Heterojunction Solar Cells: Investigations on Morphology and Performance" J. Sol. Energy Eng. 137, 031016, January 2015.

[19] A. Wanninayake, S. Gunashekar, S. Li, B. C. Church and N. Abu-Zahra," Performance enhancement of polymer solar cells using copper oxide nanoparticles"Semicond. Sci. Technol.30, 064004, May 2015

[20] F. C. Chen, J. L. Wu, C. L. Lee, Y. Hong, C. H. Kuo, and M. H. Huang, "Plasmonic-enhanced polymer photovoltaic devices incorporating solution-processable metal nanoparticles"Appl. Phys. Lett. 95, 013305, July 2009.

[21] F. X. Xie, W. C. H. Choy, C. C. D. Wang, W. E. I Sha, D. D. S. Fung,"Improving the efficiency of polymer solar cells by incorporating gold nanoparticles into all polymer layers" Appl. Phys. Lett. 99 153304, October 2011.

[22] F. X. Xie, W. C. H. Choy, X. Zhu, X. Li, Z. Li, and C. Liang," Improving polymer solar cell performances by manipulating the self-organization of polymer" Appl. Phys. Lett.98, 243302, June, 2011.

[23] S. W. Baek, J. Noh, C. H. Lee, B. Kim, M. K. Seo, J. Y. Lee, "Plasmonic Forward Scattering Effect in Organic Solar Cells: A Powerful Optical Engineering Method" Nat. Sci. Rep., 3, 1726, April 2013.

[24] X. Chen, L. Zuo, W. Fu, Q. Yan, C. Fan, H. Chen, "Insight into the efficiency enhancement of polymer solar cells by incorporating gold nanoparticles" Sol. Energy. Mat. Sol. 111, pp 1-8, April 2013.

[25] F. A. George, A. Dibb, M. A. Muth, T. Kirchartz, S. Engmann, H. Hoppe, G. Gobsch, M. Thelakkat, N. Blouin, S. Tierney, M. Carrasco Orozco, J. R. Durrant, and J. Nelson, "Influence of doping on charge carrier collection in normal and inverted geometry polymer:fullerene solar cells", Scientific Reports, 3, pp. 3335. November, 2013

[26] T. Erb, U. Zhokhavets, G. Gobsch, S. Raleva, B. Stuhn, P. Schilinsky, C. Waldauf, and C. J. Brabec, "Correlation Between Structural and Optical Properties of Composite Polymer/Fullerene Films for Organic Solar Cells" Adv. Funct. Mater.15, pp 1193-1196, July 2005.

[27] S. W. Heo, K. W. Song, K. H. Baek, T.H. Lee, J.Y. Lee and D. K. Moon, "Enhanced performance in inverted polymer solar cells via solution process: Morphology controlling of PEDOT:PSS as anode buffer layer by adding surfactants"Organic Electronics, 14, pp 1629–1635, June 2013.

[28] D. D. S. Fung, L. F. Qiao, W. C. H. Choy, C. D. Wang, W. E. I. Sha, F. X. Xie and S. He, "Optical and electrical properties of efficiency enhanced polymer solar cells with Au nanoparticles in a PEDOT–PSS layer"J. Mater. Chem. 21, pp 16349–16356, September, 2011.

[29] S. A. Choulis, Y. Kim, J. Nelson, D. D. C. Bradley, M. Giles, M. Shkunov, and I.

McCulloch, "High ambipolar and balanced carrier mobility in regioregular poly (3-hexy thiophene)". Applied Physics Letters. 85 (**17**), pp 3890-3892, October, 2004

[30] J. Choulis, A. Baumumann, A. Wagenpfahl, C. Deibel, and V. Dyakonov, Oxygen doping of P3HT: PCBM blends: Influence on trap states, charge carrier mobility and solar cell performance" Organic Electronics. 11 (**10**), pp 1693–1700, August, 2010

[31] B.P. Nguyen, T. Kim, and C.R. Park," Nanocomposite-Based Bulk Heterojunction Hybrid Solar Cells" J. Nanomater., 2014, January 2014

[32] L. Lu, Z. Luo, T. Xu, and L. Yu," Cooperative plasmonic effect of Ag and Au nanoparticles on enhancing performance of polymer solar cells" Nano Letters. 13(1), pp 59-64, December 2013.

[33] V. Jankovic, Y. M. Yang, J. You, L. Dou, Y. Liu, P. Cheung, J. P. Chang, and Y. Yang, "Active Layer-Incorporated, Spectrally Tuned Au/SiO2 Core/Shell Nanorod-Based Light Trapping for Organic Photovoltaics". ACS Nano. 7(**5**) pp 3815–3822, April, 2013.

[34] Gadisa, A., Svensson, M., Andersson, M. R., Inganäs, O., "Correlation between Oxidation Potential and Open Circuit Voltage of Composite Solar Cells based on Blends of Polythiophenes/Fullerene Derivative", Appl. Phys. Lett., 84, pp.1609−1611, February, 2004

[35] N. Kudo, Y. Shimazaki, H. Ohkita, M. Ohoka, S. Ito, "Organic–inorganic hybrid solar cells based on conducting polymer and SnO2 nanoparticles chemically modified with a fullerene derivative". Solar Energy Materials and Solar Cells. 91,(**13**),15, pp 1243–1247, August, 2007

[36] P. S. Mbule, T. H. Kim, B. S. Kimb, H. C. Swart, and O. M. Ntwaeaborw, "Effects of particle morphology of ZnO buffer layer on the performance of organic solar cell devices." Solar Energy Materials and Solar Cells 112, pp 6–12, January, 2013

[37] S. Jin, B. V. K. Naidu, H. Jeon, S. Park, J. Park, S. C. Kim, J. W. Lee, and Y. Gal, "Optimization of process parameters for high-efficiency polymer photovoltaic devices based on P3HT: PCBM system." Solar Energy Materials and Solar Cells, 91, pp 1187–1193, 2007

[38] Y. Kim, S.A. Choulis, J. Nelson, D.D.C. Bradley, S. Cook, J.R. Durrant, "Composition and annealing effects in polythiophene/fullerene solar cells". J. Mater. Sci. 40, 1371, March, 2005.

[39] F. C. Krebs, Y. Thomann, R. Thomannand J. W. Andreasen, "A simple nanostructured polymer/ZnO hybrid solar cell-preparation and operation in air"Nanotechnology19, 424013, December 2008.